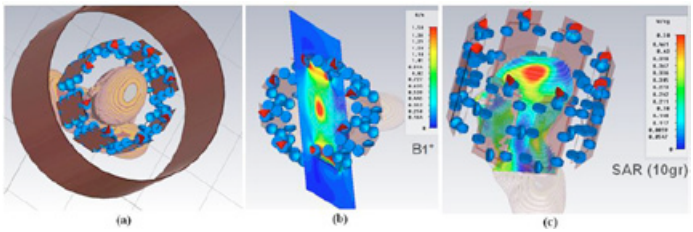

Fig.2 (a): The FDTD simulation model (b): The B^{1+}(transmit field) profile using CP^{+1} mode, (c): The point SAR distribution with distinct hotspots at the middle of brain using CP^{+1} mode

Both the reflection (S_{11}) for all channels and the transmission (S_{21}) between any two channels at 297.2 MHz was lower than -20 dB.

Fig.3 shows the measured B_1 efficiency of the array using a sugar-water phantom after phase shimming (all 8 channels) with a maximum B_1 efficiency of 0.46 [µT/sqrt{W}], whereas a maximum B_1 efficiency of 0.34 [µT/sqrt{W}] was measured in an oil phantom and of 0.33 [µT/sqrt{W}] in the human brain of a healthy volunteer respectively.

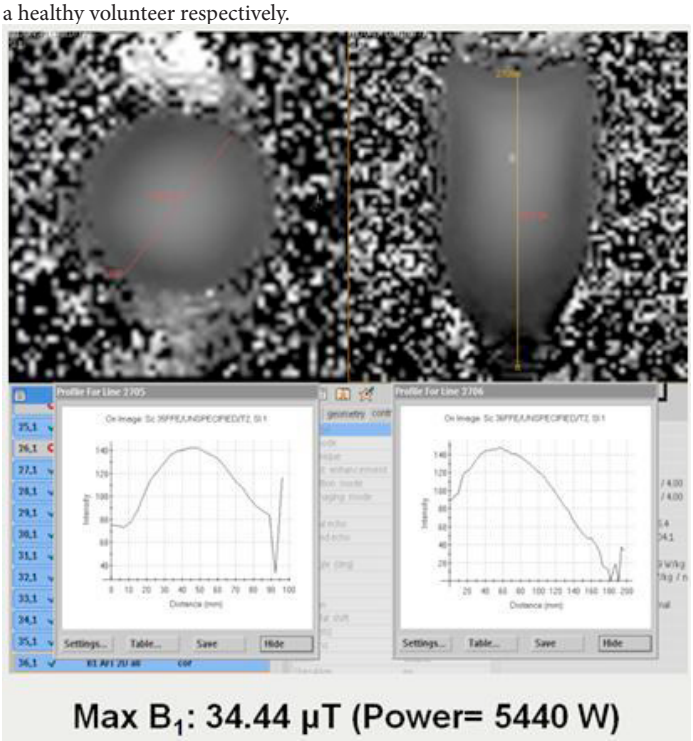

Fig.3 measured B_1 efficiency of the array using a sugar-water phantom

The noise correlation measurement of the coil (used as transceive coil array) is also shown in Fig.4. The maximum noise correlation can be seen between channels 3 and 4 (40%) when the coil loaded with an oil phantom.

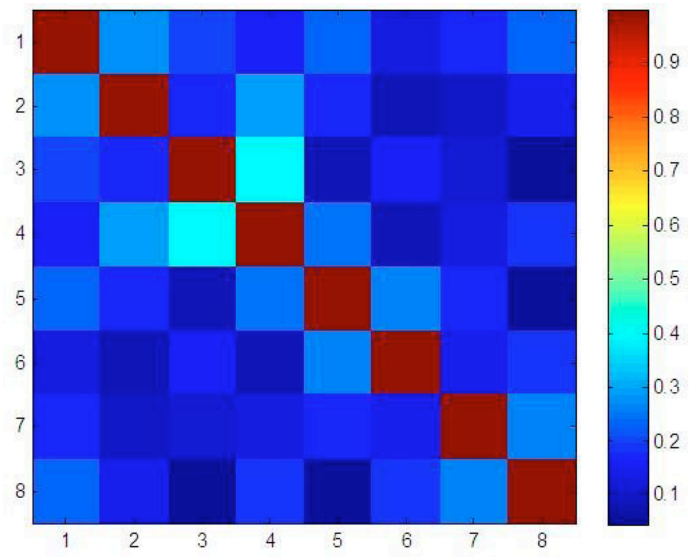

Fig.4 Noise correlation matrix

Discussion/Conclusion: An 8-channel transceive head coil was constructed and evaluated on a 7T MRI system. The optimized coil array has been shown to produce high B_1 efficiency and high SNR. This coil can be used both as a transceive coil alone (due to its high B_1 efficiency and low SAR) and also as a transmit-only coil.

References:

[1] CST: Field Simulation Software: CST MICROWAVE STUDIO 2009. http://www.cst.com

443

An intrinsically dual-tuned half-wavelength CRLH resonator for combined $^{23}Na/^{1}H$ MRI at 7T

J.T. Svejda, D. Erni, A. Rennings
General and Theoretical Electrical Engineering (ATE), University of Duisburg-Essen, Duisburg/GERMANY

Purpose/Introduction: MR-imaging with X-nuclei – like ^{13}C, ^{23}Na or ^{31}P – becomes more feasible considering ultra-high-field MRI-systems. We propose a novel intrinsically dual-tuned single-element antenna for combined $^{23}Na/^{1}H$ 7T-MRI. It exhibits a congener resonance behaviour (half-wavelength current distribution) for two distinct frequencies (79MHz for sodium and 298MHz for proton). Accordingly the single-element is termed congener dual-resonant antenna (CDRA). Conventional RF-coils like dual-tuned birdcage-coils [1] are rigid structures. The presented CDRA supports in contrast a multichannel usage and therefore RF-shimming as strip-line elements [1] do.

The CDRA is based on a 6-cell composite right-/left-handed (CRLH) transmission-line [2]. To get a half-wavelength current distribution the end of the line must be either short- or open-circuited. The open leads to a current-maximum in the middle of the CDRA; the short to maxima at both line-ends. A comparison of these two cases is also presented.

Subjects and Methods: The design process of the CDRA is composed of two steps:

1) CRLH-unit-cell optimisation with FEM-solver COMSOL [http://www.comsol.com/] and eigenfrequency-simulation.

2) Driven-mode simulation of the whole CDRA with FDTD-solver EMPIRE [http://www.empire.de/].

For the half-wavelength operation a phase-shift per cell-length *p* of 30°/70mm is required. The structure of such a CRLH-unit-cell is shown in Fig.1 with

the equivalent-circuit composed of shunt (Y_{sh}) and series (Z_{se}) resonators. Capacitances are realised by metal-insulator-metal (MIM)-structures, series-inductance parasitically and shunt-inductance with a coaxial stub-line. The used materials are specified in Table1.
All simulations include a box-shaped body-phantom 5cm above the structure (for phantom-parameters cf. Table2).

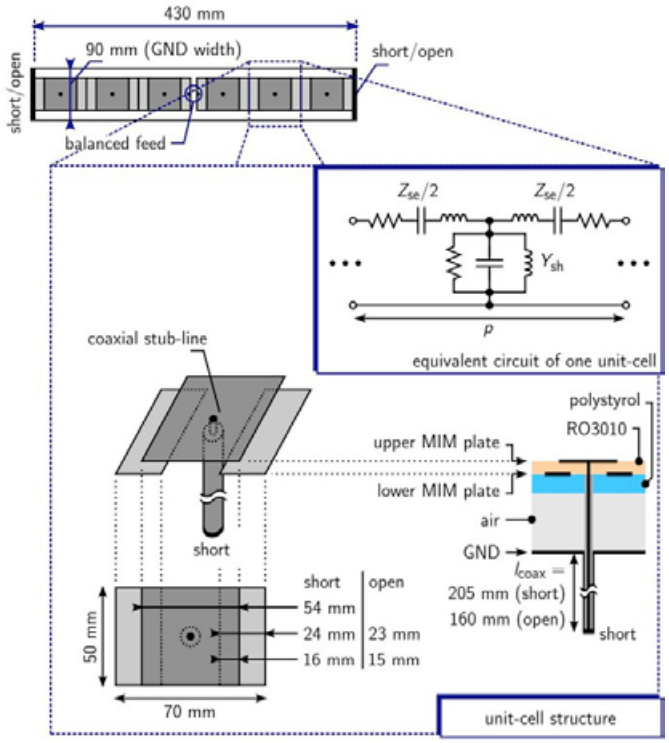

Table1: Dielectric material-properties		
	relative-permittivity	thickness
RO3010	11.2	0.25mm
Polystyrol	2.53	1.0mm
Air	1.0	5.0mm

Table2: Body-phantom-parameters	
x-dimension (longitudinal)	500mm
y-dimension (transversal)	400mm
z-dimension (transversal)	200mm
relative-permittivity	60
Conductivity	0.81S/m

Results: In Fig.2-4 FDTD-simulation results are given, including the short-/open-circuited case (left/right) at both frequencies (top/bottom). Fields are displayed logarithmically (40dB-range) normalized to the associated maxima for comparability. Fig.2 illustrates the instantaneous B_1-field inside the phantom and the J_x-component along the CDRA. Transversal B_1-field-slices along the *x*-direction are shown in Fig.3. The local specific-absorption-rate (SAR) is depicted in Fig.4.

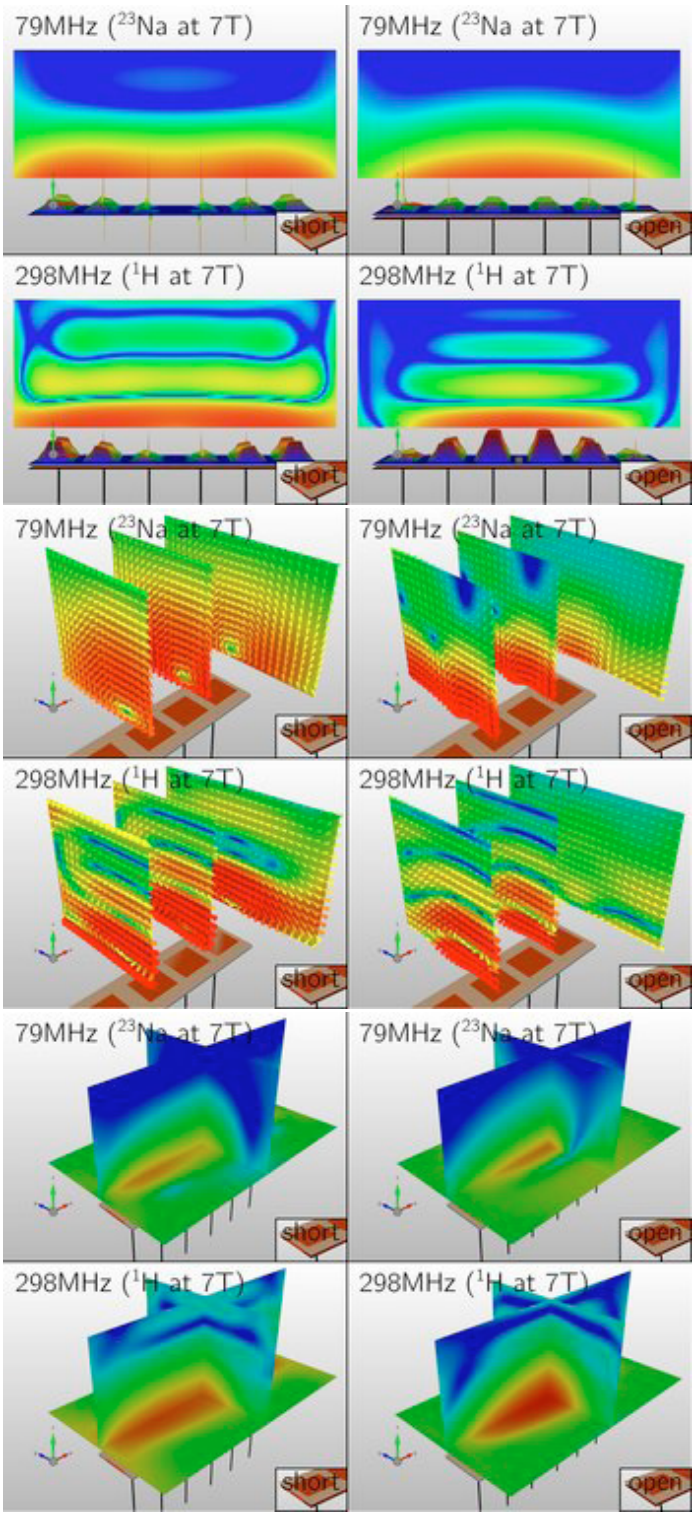

Discussion/Conclusion: The half-wavelength current distribution of short- and open-circuited CDRA is clearly recognisable in Fig.2 and Fig.3. These results reveal a better B_1-field-uniformity for the short-circuited CDRA. A further advantage of the short-circuit is the wide-spread of power-absorption which yields a smaller SAR-maximum (Fig.4). Due to their performance

and compactness, short-circuited CDRAs are best suited for multi-channel implementations.

References:

[1] Vaughan,J.T. et al.;RF Coils for MRI; UK:John Wiley&Sons;2012;137-146,169-174,197-208,378-379

[2] Caloz,C. et al.;Electromagnetic Metamaterials; USA:John Wiley&Sons;2006